Physics Letters B 784 (2018) 423–428

Contents lists available at ScienceDirect

Physics Letters B

www.elsevier.com/locate/physletb

Study of giant dipole resonance in hot rotating light mass nucleus ^{31}P

Debasish Mondal [a,*], Deepak Pandit [a], S. Mukhopadhyay [a,b], Surajit Pal [a], Srijit Bhattacharya [c], A. De [d], N. Dinh Dang [e,f], N. Quang Hung [g], Soumik Bhattacharya [a,b], S. Bhattacharyya [a,b], Balaram Dey [h], Pratap Roy [a], K. Banerjee [a,b,1], S.R. Banerjee [i]

[a] Variable Energy Cyclotron Centre, 1/AF-Bidhannagar, Kolkata 700064, India
[b] Homi Bhabha National Institute, Training School Complex, Anushaktinagar, Mumbai 400094, India
[c] Department of Physics, Barasat Government College, Kolkata 700124, India
[d] Department of Physics, Raniganj Girls' College, Raniganj 713358, India
[e] Quantum Hadron Physics Laboratory, RIKEN Nishina Center for Accelerator-Based Science, RIKEN, 2-1 Hirosawa, Wako City, Saitama 351-0198, Japan
[f] Institute of Nuclear Science and Technique, Hanoi 122100, Vietnam
[g] Institute of Fundamental and Applied Sciences, Duy Tan University, Ho Chi Minh City 700000, Vietnam
[h] Saha Institute of Nuclear Physics, 1/AF-Bidhannagar, Kolkata 700064, India
[i] (Ex)Variable Energy Cyclotron Centre, 1/AF-Bidhannagar, Kolkata 700064, India

ARTICLE INFO

Article history:
Received 21 May 2018
Received in revised form 3 July 2018
Accepted 27 July 2018
Available online 30 July 2018
Editor: V. Metag

Keywords:
Isovector giant dipole resonance
Statistical theory of nucleus
BaF_2 detectors

ABSTRACT

An exclusive systematic study of the giant dipole resonance (GDR) parameters has been performed in very light mass nucleus ^{31}P in the temperature range of $\sim$ 0.8–2.1 MeV and average angular momentum of $\sim$ 11–16 $\hbar$. The high-energy γ rays from the decay of the GDR, evaporated neutrons and γ-ray multiplicities have been measured. The angular distribution of high-energy γ rays has also been measured at $E_{\rm beam} = 42$ MeV. The GDR parameters, nuclear level density parameter and nuclear temperature were precisely determined by simultaneous statistical model analysis of high-energy γ ray and evaporated neutron spectra. It is observed that the measured width remains roughly constant up to a temperature of $\sim$ 1.6 MeV. Moreover, the thermal pairing plays no role in describing the GDR width in this open-shell light nucleus at the above-mentioned temperatures and angular momenta. The present measurements provide an excellent platform to extend the applicability of the existing theoretical models down to the very light mass nuclei.

The isovector giant dipole resonance (IVGDR or commonly known as GDR) is a member of a broad family of collective resonances in nuclei called giant resonances [1,2]. Macroscopically, it is conceived as the out-of-phase oscillation of proton and neutron fluids, while microscopically, it is described as the coherent excitation of 1 particle–1 hole ($1p$–$1h$) configurations across one major shell. The short lifetime of this resonance makes it an excellent probe to study the nuclear properties at extreme conditions, e.g. nuclear shapes and deformations at high temperature and angular momentum [3–10], fission time scale [11–13], isospin mixing [14–20], the ratio of nuclear shear viscosity to entropy volume density [21,22] etc.

After the first observation of the GDR built on the nuclear excited states in heavy-ion fusion reactions nearly four decades ago [23], a great wealth of data has been accumulated over the years regarding the properties of the GDR parameters [1,24–27]. It is observed that the GDR energy remains roughly constant at the ground-state value with increasing nuclear temperature (T) and angular momentum (J), while the width increases with both T and J. It is worth mentioning, in this context, that in a heavy-ion fusion reaction, the compound nucleus (CN) is populated at high J along with the intrinsic excitation. It is, therefore, very difficult to disentangle the effects of T and J on the GDR width. Researchers have also used inelastic scattering to study the GDR [28–30]. In this case, the CN is populated at low angular momentum but with a broad range of excitation energy. Another excellent technique to study the exclusive temperature dependence of the GDR is using the light-ion induced fusion reaction, in which the CN is populated at a definite initial excitation energy and a small distribution of J as compared to that obtained in the heavy-ion

* Corresponding author.
E-mail address: debasishm@vecc.gov.in (D. Mondal).
[1] Present address: Department of Nuclear Physics, Research School of Physics and Engineering, The Australian National University, ACT0200, Australia.

https://doi.org/10.1016/j.physletb.2018.07.052

reaction. Moreover, the average angular momentum remains much smaller than the critical angular momentum $J_c = 0.6A^{5/6}$ [31], above which the effect of J on the GDR width is observed. This technique has recently been utilized in a series of experiments [32–34] to exclusively probe the variation of the GDR width with temperature. The main disadvantage of this technique is the presence of non-statistical bremsstrahlung radiation, which has to be properly accounted for.

Various models have been proposed to explain the observed increase in the GDR width with T and J. The thermal shape fluctuation model (TSFM), which was widely used to describe the experimental measurements, states that, at a given T and J, the GDR line shape is the superposition of the line shapes of an ensemble of nuclei having different deformations [35–39]. This model predicts the J dependence quite well. However, it deviates from the measured data at low as well as high temperatures. At low temperatures, it is observed that the GDR width remains at the ground-state value up to $T \sim 1$ MeV and increases thereafter [33,34], whereas at high temperatures ($T > 2.5$ MeV) the width saturation of the GDR is still under debate [40–44]. In this context, it should be highlighted that, by including the thermal pairing in the TSFM calculations, the GDR width has recently been fairly well described at $T < 1.5$ MeV in open-shell nuclei [45]. Interestingly, the microscopic phonon damping model (PDM) [46,47], which states that the GDR width arises owing to the coupling of the GDR state to the non-collective *ph* states (quantal width) as well as *pp* and *hh* states (thermal width), describes the measured width quite well at both low and high T, where it predicts a saturation of the GDR width. Recently, a phenomenological model, called critical temperature included fluctuation model (CTFM), has been proposed [33]. According to this model, the GDR width remains constant up to a critical temperature and increases thereafter. This model also reproduces the GDR width at low as well as high T and J quite well [33,34,48,49].

The conclusions drawn so far are mainly based on the experimental studies in medium and heavy mass nuclei in which the GDR strength is well concentrated. However, very few experiments exist below the mass $A \sim 100$ [7,34,44,49–54] and, especially below $A \sim 50$ [55], where the GDR is characterized by its own prominent features, e.g. configurational splitting [56], isospin splitting [57,58], etc. In this mass region there are some studies related to isospin mixing at high temperatures [14–20] and Jacobi shape transitions [59–64]. However, an exclusive and systematic study of the variation of the GDR parameters with T and J is still absent.

In this Letter, we present the first exclusive study of the GDR width in $A \sim 30$ mass region, utilizing the light-ion beam (α). The GDR and nuclear level density (NLD) parameters have been determined properly by simultaneous statistical model analysis of the measured high-energy γ ray and neutron spectra. The angular momentum of the CN has been determined by measuring the low-energy γ-ray multiplicities. The angular distribution of high-energy γ rays has been performed to determine the bremsstrahlung component. The present study provides an excellent testing ground for the existing theoretical models in their application down to very light-mass nuclei.

The experiments were performed at the Variable Energy Cyclotron Centre (VECC), Kolkata. A self-supporting ^{27}Al target was bombarded with a pulsed ^{4}He beam of energies $E_{\rm beam} = 28$, 35, 42 MeV from K-130 cyclotron. The initial excitation energies of the CN ^{31}P were 34.1, 40.2, and 46.2 MeV, respectively. It should again be emphasized that, due to the availability of ^{4}He beam, ^{31}P could be populated below the critical angular momentum $J_{\rm cr} = 19\ \hbar$ [65] for the Jacobi shape transition, already observed in the same nucleus [64]. In addition, the CN was populated just above the critical angular momentum $J_{\rm c} = 10.5\ \hbar$ [31]. Therefore the effect of J on the GDR width is expected to show up. The high-energy γ rays from the decay of the GDR were measured by a part of the LAMBDA spectrometer (49 BaF_2 scintillators, each having dimensions of $3.5 \times 3.5 \times 35$ cm^3) [66] placed at a distance of 50 cm from the target position at $\theta = 90^\circ$ with respect to the beam direction. The γ-ray multiplicities were measured, in coincidence with the high-energy γ rays, with a 50-element multiplicity filter (BaF_2 scintillators, each having dimensions of $3.5 \times 3.5 \times 5$ cm^3) [67]. It was divided into two parts of 25 elements each and they were placed on the top and bottom of the target chamber in 5×5 matrix at a distance of ~ 5 cm from the target in a staggered-castle type geometry. The multiplicity filter was also employed as a start trigger for the time of flight (TOF) measurement, which was used to reject the neutron background. As the energy of the GDR is relatively large for light nuclei, the yield of γ rays is small in the GDR region. Therefore, special cares were taken to suppress the background events, especially the cosmic backgrounds. The cyclotron rf time spectrum was recorded with respect to the multiplicity filter to minimize the random coincidences. The spectrometer was surrounded by a 10 cm thick passive lead shield to block the γ-ray backgrounds. The cosmic muons were rejected by using their hit-pattern in the highly granular LAMBDA array [66]. In addition, the data were recorded only when at least one detector of the LAMBDA array above a threshold of ~ 4 MeV fired in coincidence with both the top and bottom multiplicity filters. This technique significantly reduces the background events. The angular distribution of high-energy γ rays was measured at $\theta = 55^\circ$, 90°, 125° for $E_{\rm beam} = 42$ MeV. In the off-line analysis different angular-momentum-gated high-energy γ spectra were reconstructed by the cluster summing technique [66]. The pile-up events were rejected by using the pulse shape discrimination (PSD) method performed by collecting the charge over two time gates of 50 ns (short gate) and 2 μs (long gate). The evaporated neutron energy spectra were measured, in coincidence with the γ-ray multiplicities, by using a liquid-scintillator-based neutron TOF detector [68] (5″ diameter, 5″ length), which was placed at a distance of 150 cm from the target position and at an angle of 150° with respect to the beam direction. The PSD technique comprising of the TOF and zero cross-over time (ZCT) was utilized for the $n - \gamma$ discrimination. The measured TOF spectra were converted to angular-momentum-gated neutron energy spectra by taking the prompt γ peak as a time reference. The spectra were then converted from the laboratory frame to the center of mass (CM) frame. The typical energy resolution of the present set-up is of $\sim 17\%$ at 1 MeV. The detailed energy-dependent neutron detection efficiency can be found in Ref. [68].

The angular momentum of the CN was determined from the measured fold distribution (number of multiplicity detector fired in each event) by using the GEANT simulations. A detailed simulation was necessary to account for the data recording condition (top–bottom coincidence), which selects a slightly higher angular momentum space. A triangular distribution of γ-ray multiplicities was thrown with an adjustable peak and a width, which were determined by comparing the measured and simulated fold distributions. These are shown in Fig. 1 along with the incident and different fold-gated angular momentum distributions. The details of this technique are described in Ref. [67]. The simulated angular momentum distributions were then incorporated in the statistical model code CASCADE [69]. As the isospin splitting is crucial for GDR in light nuclei, the statistical model analysis was performed by using a version of the CASCADE code, which was modified to incorporate the GDR as well as the isospin and parity quantum numbers [14,15]. The partial decay widths were calculated by us-

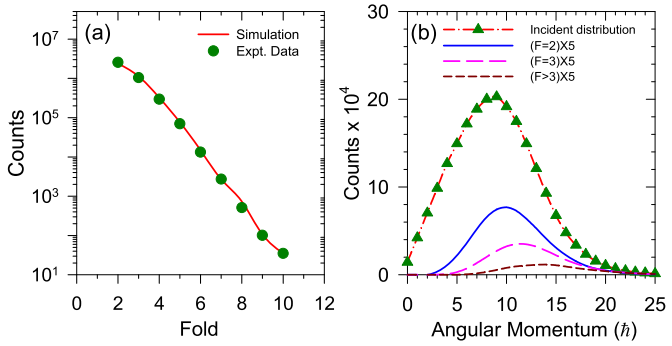

Fig. 1. (a) Experimental (green symbols) and simulated (red line) fold distributions for ^{31}P populated at initial excitation energy of 46.2 MeV. (b) Incident and different fold-gated angular momentum distributions. (For interpretation of the colors in the figure(s), the reader is referred to the web version of this article.)

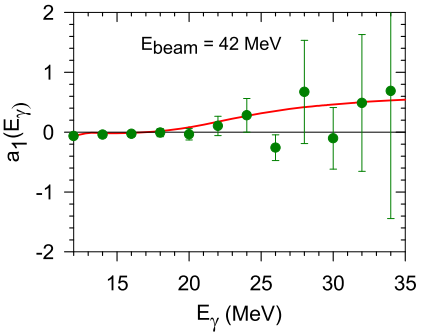

Fig. 2. Variation of $a_1(E_\gamma)$ with the γ ray energy. The green solid circles are experimentally determined, while the red solid line is theoretically calculated for $E_0 = 5.3$ MeV.

ing the reciprocity relation assuming a Lorentzian photoabsorption cross section in the inverse channel given by

$$\sigma_{\rm abs}(E_\gamma) = \frac{4\pi e^2\hbar}{m_{\rm p}c}\frac{NZ}{A}S_{\rm G}\frac{\Gamma_{\rm G}E_\gamma^2}{(E_\gamma^2 - E_{\rm G}^2)^2 + \Gamma_{\rm G}^2E_\gamma^2}, \quad (1)$$

where N and Z are the neutron and proton numbers and $m_{\rm p}$ is the proton mass. $S_{\rm G}$, $E_{\rm G}$, and $\Gamma_{\rm G}$ are the GDR fraction of total energy weighted dipole sum rule, the energy and the width, respectively. The variation of $E_{\rm G}$ along the decay cascade was properly taken care of. The GDR parameters were extracted by comparing the measured high-energy γ rays with the statistical model calculations along with a bremsstrahlung component parametrized as $\sigma = \sigma_0 \exp(-E_\gamma/E_0)$ and folded with the response function of the LAMBDA array. At $E_{\rm beam} = 42$ MeV the slope parameter E_0 was determined from the measured angular distribution of the high-energy γ rays, which is slightly forward peaked in the CM frame because of the non-statistical bremsstrahlung component. In the CM frame the γ ray angular distribution was assumed to have the form $W(E_\gamma,\theta) = W_0(E_\gamma)[1 + a_1(E_\gamma)P_1(\cos\theta) + a_2(E_\gamma)P_2(\cos\theta)]$. In the nucleon–nucleon frame of reference the bremsstrahlung was assumed to be isotropic and the slope parameter E_0 was determined by comparing the measured and calculated $a_1(E_\gamma)$ (Fig. 2). The extracted slope parameters were roughly consistent with the systematics $E_0 = 1.1[(E_{\rm beam} - V_{\rm c})/A_{\rm p}]^{0.72}$, with $V_{\rm c}$ and $A_{\rm p}$ being the Coulomb barrier and projectile mass, respectively [70]. At other beam energies, E_0 was guided by this prescription and the visual inspection of measured γ rays above $E_\gamma \sim 25$ MeV. It should be emphasized here that the main ingredient of statistical model calculations is the NLD, which was properly determined in the present study. In the CASCADE code, the level density was taken based on Fermi gas model given as

$$\rho(E^*, J) = \frac{2J+1}{12\Theta'^{3/2}}\sqrt{a}\frac{\exp(2\sqrt{aU})}{U^2}, \quad (2)$$

where $\Theta' = \Theta(1 + \delta_1 J^2 + \delta_2 J^4)$ is the deformable liquid drop moment of inertia; $\Theta = 2I_{\rm r}/\hbar^2$, $I_{\rm r} = 2/5MR^2$ is the rigid body moment of inertia and δ_1, δ_2 are the deformability coefficients. The quantity $U = E^* - \Delta - E_{\rm rot}$ is the intrinsic excitation energy with Δ and $E_{\rm rot} = J(J+1)/\Theta'$ being the pairing and rotational energies, respectively. The parameter a is the NLD parameter, which is proportional to the single particle density of states at the Fermi surface. According to the prescription by Ignatyuk and Reisdorf [71,72], the NLD parameter is given as $a = \tilde{a}(A)[1 + \frac{\Delta S}{U}\{1 - exp(-\gamma U)\}]$. Following Ref. [55], in which, the authors performed a detailed study of NLD in light-mass nuclei, the asymptotic NLD parameter was taken as $\tilde{a}(A) = 0.04543r_0^3A + 0.1246r_0^2A^{\frac{2}{3}} + 0.1523r_0A^{\frac{1}{3}}$. The numerical co-efficients for the surface and curvature terms are slightly different from those given by Reisdorf [72]. The shell damping factor γ is 0.054 MeV^{-1} [73] and the ground-state shell correction ΔS is -2.23 MeV. As $\tilde{a}$ depends on both temperature and angular momentum [73,74], it was determined by varying the r_0 parameter to match the measured neutron spectra. It should be emphasized that a given fold-gated high-energy γ and neutron spectra were analyzed simultaneously so that the GDR and the NLD parameters could be determined in a consistent way. The best-fit parameters were extracted by using the χ^2 minimization technique. The measured γ and neutron spectra along with the best-fit statistical model calculations are shown in Fig. 3. In order to emphasize the GDR region, the linearized spectra are shown in Fig. 4 by using the quantity $\sigma_{\rm abs}^{\rm exp}(E_\gamma) = \sigma_{\rm abs}(E_\gamma)Y^{\rm exp}(E_\gamma)/Y^{\rm cal}(E_\gamma)$, where $Y^{\rm exp}(E_\gamma)$ and $Y^{\rm cal}(E_\gamma)$ are the experimental and the best-fit CASCADE spectra, whereas $\sigma_{\rm abs}(E_\gamma)$ is the Lorentzian absorption cross section given by Eq. (1). The best-fit parameters are shown in Table 1. The temperature was calculated from the relation $T = \sqrt{U'/a(U')}$,

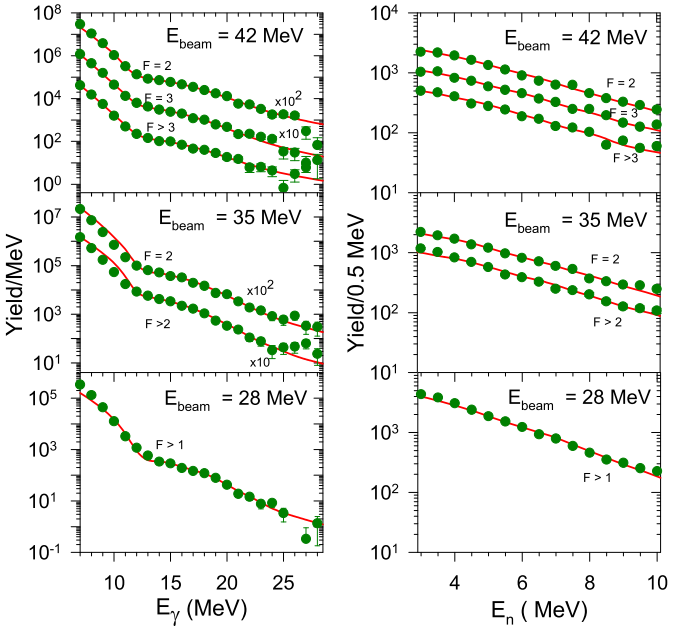

Fig. 3. Different fold-gated high-energy γ ray spectra (left panel) and the evaporated neutron energy spectra (right panel) for ^{31}P. The green solid symbols are experimentally measured spectra, while the red solid lines are the corresponding results of the statistical model calculations.

Table 1
Experimental GDR, asymptotic NLD and bremsstrahlung slope parameters at the specified angular momenta and temperatures.

E_{beam} MeV	$< J >$ $\hbar$	T MeV	$\tilde{a}$ MeV^{-1}	E_G MeV	Γ_G MeV	S_G	E_0 MeV
28	12.2 ± 4.2	0.8 ± 0.4	4.7 ± 0.2	18.7 ± 0.3	7.4 ± 0.7	1.00 ± 0.09	4.3
35	11.0 ± 3.6	1.8 ± 0.2	4.2 ± 0.2	17.1 ± 0.3	8.2 ± 0.7	0.90 ± 0.08	4.8
	13.4 ± 4.3	1.6 ± 0.3	4.2 ± 0.2	16.8 ± 0.3	7.7 ± 0.7	0.97 ± 0.09	4.8
42	11.8 ± 3.7	2.1 ± 0.2	4.3 ± 0.2	17.5 ± 0.2	9.3 ± 0.4	1.00 ± 0.05	5.3
	13.5 ± 4.1	2.0 ± 0.2	4.0 ± 0.2	17.0 ± 0.3	8.9 ± 0.7	1.00 ± 0.07	5.0
	15.9 ± 5.2	1.7 ± 0.3	4.0 ± 0.2	17.8 ± 0.3	8.5 ± 0.6	1.00 ± 0.08	5.3

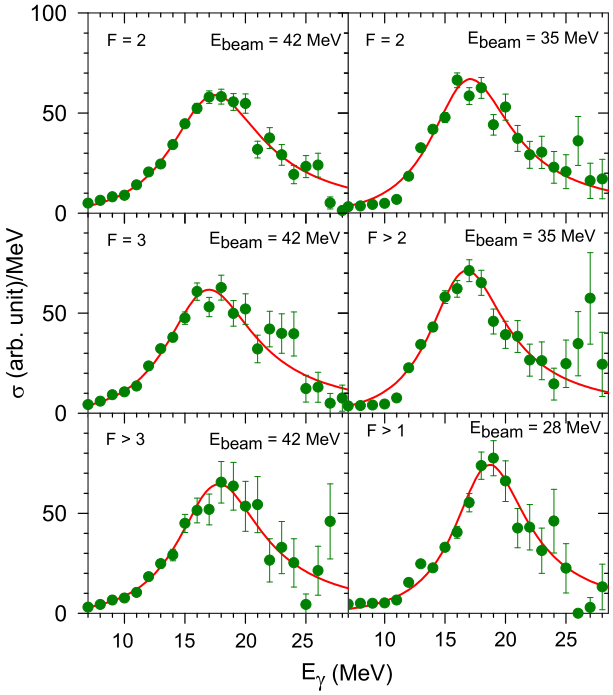

Fig. 4. Different fold-gated linearized γ ray spectra for ^{31}P. The green solid symbols are experimentally measured $\sigma_{abs}^{exp}(E_\gamma)$ (see the text), while the red solid lines are the corresponding Lorentzians having the GDR parameters as shown in Table 1.

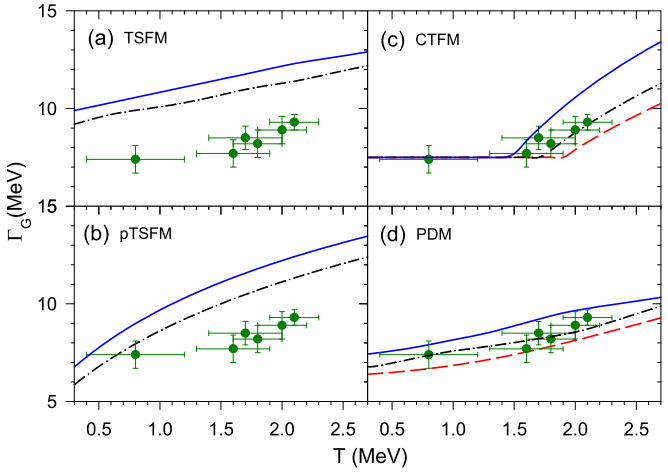

Fig. 5. Comparison of the measured GDR width with predictions by different models as a function of T at $J = 11.5\ \hbar$ (black dot-dashed line) and $J = 15.5\ \hbar$ (blue solid line) (measured range of angular momentum). The red long-dashed lines in panels (c) and (d) are the predictions at $J = 0\ \hbar$.

where $U' = E^* - E_{rot} - E_G - \Delta$. We remark here that, ^{31}P being a light nucleus, the GDR decay is predominantly from the CN and the averaging over the decay cascade reduces the temperature at the highest initial excitation energy by only 2%, which is well within the experimental errors estimated considering the uncertainties in NLD parameter, J, and E_G.

It is interesting to note that the GDR built on the excited states of ^{31}P fully exhausts the dipole strength, i.e. the GDR remains very much collective in this light nucleus. Moreover, the energy of the GDR, except at the lowest temperature, remains roughly constant at around 17.5 MeV. The slightly higher value of E_G at the lowest temperature is due to a bit higher value of the NLD parameter required for fitting the neutron evaporation spectrum. We remark here that, the measured GDR energies are lower than the ground-state value of 19.3 MeV obtained by fitting the measured photoabsorption cross section with a single Lorentzian [75]. The GDR width, on the other hand, remains roughly constant at around 7.5 MeV up to $T \sim 1.6$ MeV and gradually increases with T thereafter.

In Fig. 5 the measured GDR widths are compared with the results of calculations within different models and plotted as a function of T. As the measured angular momentum varies from 11.0–15.9 $\hbar$, the calculations have been performed for $J = 11.5$ and 15.5 $\hbar$. Moreover, the results of calculations within the CTFM and PDM have also been shown for $J = 0\ \hbar$ to visualize the explicit T dependence. Within the TSFM (Fig. 5a), the GDR apparent line shape at a given T and J was calculated as the weighted average of the various line shapes corresponding to different nuclear deformations; the weight being the Boltzmann factor $\exp(-F(\beta, \gamma', J)/T)$, where β, γ' are the deformation parameters. The free energy F was calculated considering only the deformed liquid drop energy as ^{31}P is an open-shell nucleus and the effect of the shell correction is expected to be negligible above $T \sim 1.5$ MeV [76]. It is obvious from Fig. 5a that the results of TSFM calculations overpredict the measured widths. As can also be seen from Fig. 5b, the phenomenological thermal shape fluctuation model (pTSFM) [31] fails to reproduce the measured widths even after assuming the ground-state width of ~ 3.8 MeV, which was taken for both ^{120}Sn and ^{208}Pb to describe the widths in these mass regions in Ref. [31]. Interestingly, the TSFM and pTSFM could describe the measured width above $T \sim 1.5$ MeV in medium and heavy mass nuclei. However, in the light mass region, these two models are not able to describe the measured widths even up to $T \sim 2.1$ MeV.

In Fig. 5c the CTFM calculations are presented. Within this model, the GDR width remains constant at the ground-state value up to a critical temperature $T_c = 0.7 + 37.5/A$ due to the GDR induced fluctuation and increases thereafter. In these calculations the ground-state GDR width (Γ_{gs}) for ^{31}P was taken as 7.5 MeV, which is a bit higher than the value of 6.3 MeV obtained by fitting the measured photoabsorption cross section with a single Lorentzian [75]. However, the viscous hydrodynamic model of Auerbach et al. [77] yields $\Gamma_{gs} = 7.5$ MeV and the measured data well below the critical temperature are also around this value. Hence Γ_{gs} was taken as 7.5 MeV. Interestingly, the CTFM reproduces the trend of measured GDR widths quite well with T_c of ~ 1.9 MeV predicted by the systematics. It is also interesting to note that the effect of

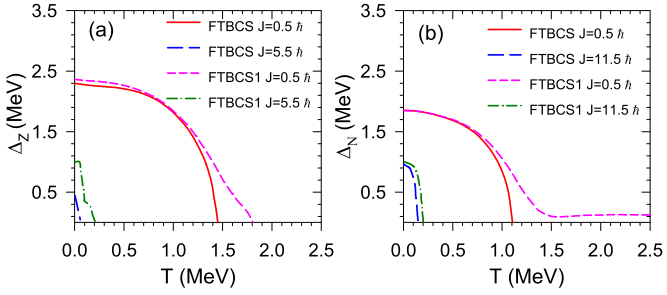

Fig. 6. (a) Proton and (b) neutron pairing gaps as functions of temperature at different angular momenta calculated within BCS and BCS1 (see text).

J increases the GDR width from the ground-state value before the critical temperature.

The measured GDR widths are compared with the results of the microscopic PDM calculations performed as a function of T and J without the inclusion of thermal pairing (Fig. 5d). Regarding the latter, the calculations within the BCS theory as well as the BCS1 one, which includes the quasiparticle number fluctuation, at finite T and J [78] were carried out. The parameters G_Z for proton and G_N for neutron pairing interactions were chosen so that the values of the corresponding pairing gaps (Δ_Z and Δ_N) at $T = 0$ are 2.3 MeV and 1.85 MeV, respectively, based on the odd–even mass differences. The results of calculations show that increasing T and J breaks the pairs so that no pairing gaps remain at $T > 0.25$ MeV and $J > 11.5\ \hbar$ (Fig. 6). This allows us to carry out the PDM calculations without thermal pairing. The single-particle energies for protons and neutrons were calculated within the deformed Wood–Saxon potentials with $\beta = 0.1$ obtained by fitting the photoabsorption cross section using the prescription of Junghans et al. [79]. The two parameters F_1 and F_2 for the coupling of the GDR to the non-collective ph and pp (or hh) configurations, respectively, were chosen so that the width of the GDR obtained at $T = 0$ and $J = 0\ \hbar$ is equal to around 6.3 MeV (the experimental ground-state GDR width), whereas its value at $T = 0.8$ MeV and $J = 11.5\ \hbar$ matches the corresponding experimental data point. The values of these parameters are kept unchanged throughout the calculations at all T and J. The GDR energy at $J = 0\ \hbar$ is set equal to ground-state value of 19.3 MeV, whereas at $J \neq 0\ \hbar$ it is 18.0 MeV comparable to the experimental values. As the agreement between theory and experiment is fairly good, it could be inferred that, pairing plays no role in the present light nucleus, leaving only the effect of angular momentum on the GDR width in it. It should be highlighted here, that both CTFM and the PDM could describe the GDR width as a function of T and J for medium and heavy mass nuclei and present work points towards the universality of these models.

In summary, an exclusive, systematic measurement of the GDR parameters has been performed using the light-ion α beam in very light-mass nucleus ^{31}P. The angular momentum of the CN has been precisely determined by measuring the low-energy γ-ray multiplicities. The GDR, nuclear level density parameters and nuclear temperatures have been accurately determined from a simultaneous statistical model analysis of the measured high-energy γ spectra and the neutron spectra. The experimentally extracted widths remains roughly constant up to 1.6 MeV temperature and gradually increases thereafter. The measured widths could be described very well within the CTFM and PDM, thereby asserting their universality in describing GDR width as a function of temperature and angular momentum. Moreover, the paring gaps are found to vanish in the ranges of T and J considered in this experiment, therefore, have no effect on the measured GDR width contrary to that observed in medium and heavy open-shell nuclei.

Acknowledgements

The authors are thankful to VECC cyclotron staffs for smooth running of the accelerator during the experiment. The PDM-related calculations were performed on the RIKEN HOKUSAI-GreatWave System and supported by the Vietnam National Foundation for Science and Technology Development under the Grant No. 103.04-2017.69.

References

[1] M.N. Harakeh, A. van der Would, Giant Resonances: Fundamental High-Frequency Mode of Nuclear Excitation, Clarendon Press, Oxford, 2001.
[2] P.F. Bortignon, A. Bracco, R.A. Broglia, Giant Resonances: Nuclear Structure at Finite Temperature, Harwood Academic Publishers, Amsterdam, 1998.
[3] J.J. Gaardhøje, et al., Phys. Rev. Lett. 53 (1984) 148.
[4] C.A. Gossett, et al., Phys. Rev. Lett. 54 (1985) 1486.
[5] D.R. Chakrabarty, et al., Phys. Rev. Lett. 58 (1987) 1092.
[6] A. Stolk, et al., Phys. Rev. C 40 (1989) R2454.
[7] J.H. Gundlach, et al., Phys. Rev. Lett. 65 (1990) 2523.
[8] R.F. Noorman, et al., Phys. Lett. B 292 (1992) 257.
[9] J.P.S. van Schagen, et al., Phys. Lett. B 308 (1993) 231.
[10] Deepak Pandit, et al., Phys. Rev. C 87 (2013) 044325.
[11] M. Thoennessen, et al., Phys. Rev. Lett. 59 (1987) 2860.
[12] P. Paul, et al., Annu. Rev. Nucl. Part. Sci. 44 (1994) 65.
[13] I. Diószegi, et al., Phys. Rev. C 63 (2000) 014611.
[14] M.N. Harakeh, et al., Phys. Lett. B 176 (1986) 297.
[15] J.A. Behr, et al., Phys. Rev. Lett. 70 (1993) 3201.
[16] M. Kicińska-Habior, et al., Nucl. Phys. A 731 (2004) 138.
[17] E. Wójcik, et al., Acta Phys. Pol. B 38 (2007) 1469.
[18] A. Corsi, et al., Phys. Rev. C 84 (2011) 041304(R).
[19] S. Ceruti, et al., Phys. Rev. Lett. 115 (2015) 222502.
[20] Debasish Mondal, et al., Phys. Lett. B 763 (2016) 422.
[21] N.D. Dang, Phys. Rev. C 84 (2011) 034309.
[22] Debasish Mondal, et al., Phys. Rev. Lett. 118 (2017) 192501.
[23] J.O. Newton, et al., Phys. Rev. Lett. 46 (1981) 1383.
[24] K.A. Snover, Annu. Rev. Nucl. Part. Sci. 36 (1986) 545.
[25] J.J. Gaardhøje, Annu. Rev. Nucl. Part. Sci. 42 (1992) 483.
[26] A. Schiller, et al., At. Data Nucl. Data Tables 93 (2007) 549.
[27] D.R. Chakrabarty, et al., Eur. Phys. J. A 52 (2016) 143.
[28] E. Ramakrishnan, et al., Phys. Rev. Lett. 76 (1996) 2025.
[29] T. Baumann, et al., Nucl. Phys. A 635 (1998) 428.
[30] P. Heckman, et al., Phys. Lett. B 555 (2003) 43.
[31] Dimitri Kusnezov, et al., Phys. Rev. Lett. 81 (1998) 542.
[32] S. Mukhopadhyay, et al., Phys. Lett. B 709 (2012) 9.
[33] Deepak Pandit, et al., Phys. Lett. B 713 (2012) 434.
[34] Balaram Dey, et al., Phys. Lett. B 731 (2014) 92.
[35] M. Gallardo, et al., Phys. Lett. B 191 (1987) 222.
[36] J.M. Pacheco, et al., Phys. Rev. Lett. 61 (1988) 294.
[37] Y. Alhassid, et al., Phys. Rev. Lett. 61 (1988) 1926.
[38] O.E. Ormand, et al., Phys. Rev. Lett. 77 (1996) 607.
[39] P. Arumugam, et al., Phys. Rev. C 69 (2004) 054313.
[40] A. Bracco, et al., Phys. Rev. Lett. 62 (1989) 2080.
[41] G. Enders, et al., Phys. Rev. Lett. 69 (1992) 249.
[42] M.P. Kelly, et al., Phys. Rev. Lett. 82 (1999) 3404.
[43] O. Wieland, et al., Phys. Rev. Lett. 97 (2006) 012501.
[44] M. Ciemala, et al., Phys. Rev. C 91 (2015) 054313.
[45] A.K. Rhine Kumar, et al., Phys. Rev. C 91 (2015) 044305.
[46] N.D. Dang, et al., Phys. Rev. Lett. 80 (1998) 4145.
[47] N.D. Dang, et al., Nucl. Phys. A 636 (1998) 427.
[48] C. Ghosh, et al., Phys. Rev. C 94 (2016) 014318.
[49] S. Ceruti, et al., Phys. Rev. C 95 (2017) 014312.
[50] M. Kicińska-Habior, et al., Phys. Rev. C 36 (1987) 612.
[51] G. Viesti, et al., Phys. Rev. C 40 (1989) R1570.
[52] M. Kicińska-Habior, et al., Phys. Rev. C 45 (1992) 569.
[53] Z.M. Drebi, et al., Phys. Rev. C 52 (1995) 578.
[54] S.K. Rathi, et al., Phys. Rev. C 67 (2003) 024603.
[55] M. Kicińska-Habior, et al., Phys. Rev. C 41 (1990) 2075.
[56] R.A. Eramzhyan, et al., Phys. Rep. 136 (1986) 229.
[57] S. Fallieros, et al., Nucl. Phys. A 147 (1970) 593.
[58] J.D. Vergados, Nucl. Phys. A 239 (1975) 271.
[59] M. Kicińska-Habior, et al., Phys. Lett. B 308 (1993) 225.
[60] A. Maj, et al., Nucl. Phys. A 731 (2004) 319.
[61] M. Kmiecik, et al., Acta Phys. Pol. B 36 (2005) 1169.
[62] Deepak Pandit, et al., Phys. Rev. C 81 (2010), 061302(R).
[63] D.R. Chakrabarty, et al., Phys. Rev. C 85 (2012) 044619.
[64] Balaram Dey, et al., Phys. Rev. C 97 (2018) 014317.

[65] W.D. Myers, et al., Acta Phys. Pol. B 32 (2001) 1033.
[66] S. Mukhopadhayay, et al., Nucl. Instrum. Methods A 582 (2007) 603.
[67] Deepak Pandit, et al., Nucl. Instrum. Methods A 624 (2010) 148.
[68] K. Banerjee, et al., Nucl. Instrum. Methods A 608 (2009) 440.
[69] F. Puhlhofer, Nucl. Phys. A 280 (1977) 267.
[70] H. Nifenecker, J.A. Pinston, Annu. Rev. Nucl. Part. Sci. 40 (1990) 113.
[71] A.V. Ignatyuk, et al., Sov. J. Nucl. Phys. 21 (1975) 255; Yad. Fiz. 21 (1975) 485.
[72] W. Reisdorf, Z. Phys. A 300 (1981) 227.
[73] Pratap Roy, et al., Phys. Rev. C 94 (2016) 064607.
[74] Pratap Roy, et al., Phys. Rev. C 86 (2012) 044622.
[75] A.V. Varlamov, et al., Atlas of Giant Dipole Resonances, INDC(NDS)-394, 1991; L. Katz, et al., Can. J. Phys. 29 (1951) 518.
[76] Deepak Pandit, et al., Phys. Rev. C 95 (2017) 034301.
[77] N. Auerbach, et al., Ann. Phys. (NY) 95 (1975) 35.
[78] N. Quang Hung, et al., Phys. Rev. C 78 (2008) 064315.
[79] A.R. Junghans, et al., Phys. Lett. B 670 (2008) 200.